

Determination of the Dominant Catalyst Derived from the Classic $[\text{RhCp}^*\text{Cl}_2]_2$ Precatalyst System: Is it Single-Metal Rh_1Cp^* -Based, Subnanometer Rh_4 Cluster-Based, or $\text{Rh}(0)_n$ Nanoparticle-Based Cyclohexene Hydrogenation Catalysis at Room Temperature and Mild Pressures?

Ercan Bayram,^{†,⊥} John C. Linehan,^{*,‡} John L. Fulton,[‡] Nathaniel K. Szymczak,[§] and Richard G. Finke^{*,†}

[†]Department of Chemistry, Colorado State University, Fort Collins, Colorado 80523, United States

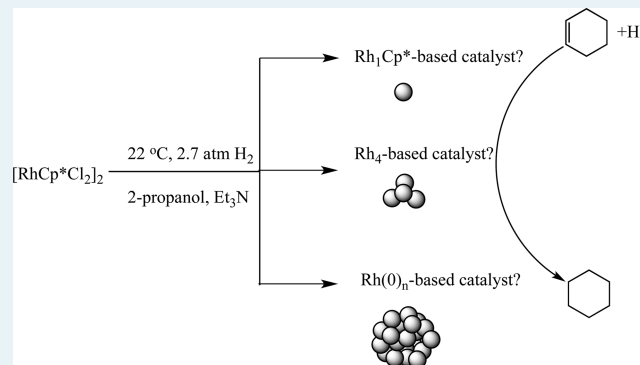
[‡]Pacific Northwest National Laboratory, Richland, Washington 99352, United States

[§]Department of Chemistry, University of Michigan, Ann Arbor, Michigan 48109, United States

Supporting Information

ABSTRACT: Determining the kinetically dominant catalyst in a given catalytic system is a forefront topic in catalysis. The $[\text{RhCp}^*\text{Cl}_2]_2$ ($\text{Cp}^* = [\eta^5\text{-C}_5(\text{CH}_3)_5]$) system pioneered by Maitlis and co-workers is a classic precatalyst system from which homogeneous mononuclear Rh_1 , subnanometer Rh_4 cluster, and heterogeneous polymetallic $\text{Rh}(0)_n$ nanoparticle have all arisen as viable candidates for the true hydrogenation catalyst, depending on the precise substrate, H_2 pressure, temperature, and catalyst concentration conditions. Addressed herein is the question of whether the prior assignment of homogeneous, mononuclear Rh_1Cp^* -based catalysis is correct, or are trace Rh_4 subnanometer clusters or possibly $\text{Rh}(0)_n$ nanoparticles the dominant, actual cyclohexene hydrogenation catalyst at 22 °C and 2.7 atm initial H_2 pressure? The observation herein of Rh_4 species by in operando-X-ray absorption fine structure (XAFS) spectroscopy, at the only slightly more vigorous conditions of 26 °C and 8.3 atm H_2 pressure, and the confirmation of Rh_4 clusters by ex situ mass spectroscopy raises the question of the dominant, room temperature, and mild pressure cyclohexene hydrogenation catalyst derived from the classic $[\text{RhCp}^*\text{Cl}_2]_2$ precatalyst pioneered by Maitlis and co-workers. Ten lines of evidence are provided herein to address the nature of the true room temperature and mild pressure cyclohexene hydrogenation catalyst derived from $[\text{RhCp}^*\text{Cl}_2]_2$. Especially significant among those experiments are quantitative catalyst poisoning experiments, in the present case using 1,10-phenanthroline. Those poisoning studies allow one to distinguish mononuclear Rh_1 , subnanometer Rh_4 cluster, and $\text{Rh}(0)_n$ nanoparticle catalysis hypotheses. The evidence obtained provides a compelling case for a mononuclear, Rh_1Cp^* -based cyclohexene hydrogenation catalyst at 22 °C and 2.7 atm H_2 pressure. The resultant methodology, especially the quantitative catalyst poisoning experiments in combination with in operando spectroscopy, is expected to be more broadly applicable to the study of other systems and the “what is the true catalyst?” question.

KEYWORDS: catalysis, determination of the dominant catalyst, catalyst poisoning studies, rhodium, organometallic complex catalysis, subnanometer cluster catalysis, nanoparticle catalysis, XAFS, in operando spectroscopic studies



INTRODUCTION

Identification of the kinetically dominant catalyst in many, if not most, catalyst systems is a challenging to often perplexing issue in catalysis science.^{1–5} The precise nature of the actual catalyst in a given catalytic reaction is a central, forefront topic in catalysis because each of the key catalytic properties of catalytic activity, selectivity, stability, poisoning, recovery, regeneration, and also catalyst optimization each depends on the identity of the kinetically dominant, “true” catalyst. Each of the above catalyst properties is inherently different for single

metal M_1 vs subnanometer M_4 vs $\text{M}(0)_n$ nanoparticle catalysts ($\text{M} = \text{transition metal}$),^{1–5} three possible catalyst types relevant to the present study.

Recently, benzene hydrogenation beginning with $[\text{RhCp}^*\text{Cl}_2]_2$ at 100 °C and 50 atm initial H_2 pressure was shown to be catalyzed by ligated- Rh_4 subnanometer clusters

Received: February 13, 2015

Revised: April 20, 2015

Published: May 27, 2015

(hereafter abbreviated for convenience as just “Rh₄”) of average formula Rh₄Cp*_{2.4}Cl₄H_c.⁶ The evidence in support of ligated-Rh₄-based catalysis included (i) in operando XAFS spectroscopy;⁷ (ii) kinetics; and crucially, (iii) 1,10-phenanthroline quantitative kinetic poisoning experiments.⁶ In operando XAFS of the benzene hydrogenation system revealed that 98 ± 2% of the starting [RhCp*Cl₂]₂ Rh mass is present as Rh₄ clusters under the 100 °C and 50 atm initial H₂ pressure catalysis conditions.⁶ Quantitative kinetic poisoning experiments revealed that the catalyst was poisoned by 4.0 ± 0.4 equiv of 1,10-phenanthroline per total equiv of Rh present, results consistent with Rh₄ subnanometer cluster catalysis. The poisoning evidence proved crucial because control experiments revealed that if even a small amount (1.4% based on total rhodium concentration) of Rh(0)_n nanoparticles had been formed (using polyethylene glycol/dodecylether hydrosol-stabilized Rh(0)_n as model nanoparticles), then that 1.4% level of Rh(0)_n nanoparticles would have been able to carry all the observed catalytic activity, the Rh(0)_n nanoparticles being ~70-fold more active than the Rh₄ clusters. However, the Rh(0)_n nanoparticles were poisoned by just 0.12 ± 0.02 equiv of 1,10-phenanthroline per total equiv of Rh present. That poisoning evidence, along with the crucial demonstration of a higher binding constant for the 1,10-phenanthroline to the Rh(0)_n nanoparticles compared to the Rh₄ subnanometer clusters,⁸ provided a compelling case for Rh₄ subnanometer benzene hydrogenation catalysis at 100 °C and 50 atm initial H₂ pressure.⁶

In contrast, for cyclohexene hydrogenation beginning, again, with [RhCp*Cl₂]₂ under the milder conditions of 22 °C and 2.7 atm initial H₂ pressure, Maitlis’s early kinetic and mechanistic studies provided good evidence at the time for [Rh₁Cp*(H)₂(solvent)] as the proposed, Rh₁Cp*-based homogeneous catalyst.⁹ In a subsequent 2005 study¹⁰ in collaboration with Prof. Maitlis, we provided six lines of evidence that appeared to strongly suggest Rh₁Cp*-based homogeneous, cyclohexene hydrogenation catalysis: (i) the catalysis starts immediately, without any observable induction period (i.e., during which other nuclearity species could have been formed); (ii) the reaction solution remains dark red during the hydrogenation and does not turn black (as expected¹ if Rh(0)_n nanoparticles were formed), nor are any metal precipitates observed at the end of the reaction (as is often seen if poorly stabilized M(0)_n nanoparticles are formed); and (iii) filtering the product solution via a 0.2 μm nylon syringe filter and then employing that filtrate in a subsequent cyclohexene hydrogenation reaction yielded a kinetically competent catalyst solution (i.e., thereby ruling out catalysis by filterable heterogeneous metal particles). Additional evidence gathered at the time consistent with Rh₁Cp*-based homogeneous catalysis included (iv) the lack of any detectable effect on the catalytic activity post the addition, when ~1/3 of the reaction was complete, of ~300 equiv of Hg(0) per total rhodium, evidence traditionally interpreted¹ as arguing against M(0)_n nanoparticle heterogeneous catalysis; (v) the report by Collman and co-workers using a polymer-bound substrate implying the presence of a homogeneous catalyst;¹¹ and importantly, (vi) the previously reported kinetic evidence and rate law provided by Maitlis and co-workers⁹ that is consistent with Rh₁Cp*-based homogeneous catalysis, notably the half-order dependence on the starting, dimeric [RhCp*Cl₂]₂ resting state en route to a postulated [Rh₁Cp*(H)₂(solvent)] catalyst (see Figure 2 in Maitlis’s paper⁹).

Although the above detailed six lines of evidence, especially Maitlis and co-workers’ kinetic and mechanistic evidence⁹ and the Hg(0) poisoning, is highly suggestive of a Rh₁Cp*-based homogeneous cyclohexene hydrogenation catalyst, four questions remained regarding [RhCp*Cl₂]₂ precatalyst-based cyclohexene hydrogenation at 22 °C and 2.7 atm initial H₂ pressure. First and foremost, (i) can the recently precedented⁶ alternative hypothesis of trace Rh₄ subnanometer cluster catalysis be definitively ruled out? Second, (ii) can quantitative 1,10-phenanthroline kinetic poisoning experiments differentiate a homogeneous, Rh₁Cp*-based catalyst from a Rh₄ subnanometer cluster catalyst? Third, (iii) if the quantitative poisoning experiments work, can one detect the poisoned catalyst via a physical characterization method, such as mass spectroscopy (MS), thereby confirming where the poison actually goes and strengthening the poisoning evidence? Only rarely has the poisoned catalyst been detected in mechanistic studies aimed at determining the kinetically dominant catalyst, Morris and co-workers’ work being an important and notable exception.¹² Finally, (iv) can the classic, albeit often problematic to perform and interpret,¹ qualitative Hg(0) poisoning test be used as well to distinguish Rh₁ catalysis from either or both Rh₄ subnanometer cluster and from Rh(0)_n nanocluster catalysis?

Noteworthy here is that the case of catalysis from Maitlis’s classic [RhCp*Cl₂]₂ precatalyst merits special attention, with, in our view, as complete studies of this prototype system as possible, because (i) it is a state-of-the-art system in which three types of catalysis are quite plausible—Rh₁Cp*-, Rh₄-, and Rh(0)_n-based catalysis—depending on the precise substrate and conditions; (ii) there is an established change from homogeneous catalysis to heterogeneous, Rh(0)_n nanoparticle catalysis on going from room to 100 °C temperature;^{6,9,10} and (iii) the possibility of M₄ subnanometer catalysis is a relatively recent development (M = Rh in the present case),⁶ one which adds yet another level of complexity to definitive determinations of the kinetically dominant catalyst when beginning with simple, stable organometallic precatalysts such as [RhCp*Cl₂]₂. In short, the [RhCp*Cl₂]₂ precatalyst system is arguably the classic, prototype system for development of the needed methodology to answer the “what is the true catalyst?” question when considering catalysis under reductive conditions.

Presented herein are studies that address the four questions raised above and that arguably complete the methodology needed to distinguish Rh₁Cp*- from Rh₄-, from Rh(0)_n-based catalysis. The additional evidence includes (i) initial in operando-XAFS studies (at 26 °C and 8.3 atm initial H₂ pressure), and independent ex situ precatalyst product analysis by MS and UV-vis (post 22–62 °C and 2.7–3.4 atm initial H₂ pressure catalysis), work that provides evidence that detectable Rh₄ subnanometer clusters do form under at least slightly more vigorous conditions; (ii) quantitative 1,10-phenanthroline poisoning experiments with both Rh₁Cp*- and Rh₄-based catalysts; (iii) MS analysis of the 1,10-phenanthroline-poisoned catalyst showing that the added 1,10-phenanthroline poison binds to a Rh₁Cp*-based backbone; and (iv) qualitative Hg(0) poisoning experiments with both Rh₁Cp*- and Rh₄-based catalysts. The new data plus key parts of the prior literature combine to provide 10 lines of complementary, compelling evidence that a Rh₁Cp*-based homogeneous catalysts is, as Maitlis first suggested,⁹ indeed, the true cyclohexene hydrogenation catalyst derived from [RhCp*Cl₂]₂ at 22 °C and 2.7 atm initial H₂ pressure. As such, a classic system is in hand in which single metal M₁ vs M₄ subnanometer vs M(0)_n

nanocluster ($M =$ transition metal) catalysis can be distinguished, including as a function of key reaction conditions, such as the substrate, temperature, pressure, and precatalyst concentration, conditions that change the kinetically dominant catalyst. A key contribution from the present studies is the relative ease and often definitive evidence from the proper catalyst poisoning experiments, herein poisoning experiments employing 1,10-phenanthroline, in conjunction with in operando spectroscopy.

EXPERIMENTAL SECTION

Materials. All commercially obtained compounds were used as received unless indicated otherwise. 2-Propanol (Aldrich, 99.5%, anhydrous, packaged under N_2) and 1,10-phenanthroline (Aldrich, 99%) were transferred into a drybox and used as received. Elemental Hg(0) (Aldrich, 99.9995%) was used in the drybox. Triethylamine (Aldrich, 99.5%, packaged under N_2) was stored in a refrigerator and used as received. Deuterated NMR solvents were purchased from Cambridge Isotope Laboratories, Inc. $[RhCp^*Cl_2]_2$ (99%) was purchased from Strem Chemicals, stored in the drybox, and used as received. Cyclohexene (99%, inhibitor-free) was purified in a MicroSolv solvent purification system (Innovative Technology) equipped with an activated $\gamma-Al_2O_3$ column under N_2 . H_2 gas was purchased from General Air (>99.5%) and was passed through a Trigon moisture trap and a Trigon Technologies oxygen/moisture trap to remove O_2 and H_2O , followed by a Trigon Technologies high capacity indicating oxygen trap. The conversion of cyclohexene to cyclohexane was verified by 1H NMR on a sample prepared by mixing 0.1 mL of the product solution into 1 mL CD_2Cl_2 and examined by Varian INOVA-300 instrument, 300.115 MHz for 1H (cyclohexene: 5.5 ppm (m), 2 ppm (m), 1.6 ppm (m); cyclohexane: 1.4 ppm (s)). Mass spectroscopy analyses were performed with the expert assistance of Don Dick of the Department of Chemistry, Central Instrument Facility, Colorado State University, via Agilent Technologies 6220 time-of-flight mass spectroscopy. UV-vis analyses were performed via Hewlett-Packard 8452A diode array spectrophotometer with UV-vis Chem Station software.

Hydrogenation Apparatus. All the hydrogenation reactions were carried out on the previously described, custom-built pressurized hydrogenation apparatus, which allows precise monitoring of the H_2 pressure decrease accompanying hydrogenations ($\pm 6.8 \times 10^{-4}$ atm) in real-time via a PC employing a LabView version 8.2 interface.^{13–16} A Fischer-Porter (F-P) bottle was connected via its Swagelok TFE-sealed Quick Connects to the hydrogenation line equipped with an Omega D1521 10 V A/D converter with RS-232 connection to a PC. Once the pressure-transducer H_2 uptake data were obtained, the data were converted to cyclohexene loss data via the known 1:1 H_2 /cyclohexene stoichiometry, and those data were plotted (such as the one shown in Figure 1, *vide infra*).¹⁷

Standard Conditions Cyclohexene Hydrogenation Reaction Beginning with $[RhCp^*Cl_2]_2$ at 22–62 °C and 2.7–3.4 atm Initial H_2 Pressure. A previously reported¹⁰ standard conditions cyclohexene hydrogenation procedure was employed. Briefly, in the drybox, 16 ± 1 mg of $[RhCp^*Cl_2]_2$ (0.026 mmol) was weighed into a 2-dram glass vial and added into a new, disposable 22 × 175 mm Pyrex culture tube with a new 5/8 × 5/16 in. Teflon-coated stir bar. Then, 9.0 mL of 2-propanol, 1.0 mL of cyclohexene, and 0.11 mL of triethylamine¹⁸ were added via separate gastight syringes. The resulting

solution was orange-red with some undissolved $[RhCp^*Cl_2]_2$. The culture tube was then placed in a F-P bottle and sealed while still in the drybox, and then the F-P bottle was removed from the drybox, placed into a constant temperature circulating bath at 22 °C (or 26 °C, where noted), and attached via Swagelok TFE-sealed Quick-Connects to the hydrogenation line (which had already been evacuated >30 min to remove trace O_2 and H_2O , followed by refilling with 2.7 (or 3.4 atm, where noted) of purified H_2). Stirring was started at 600 rpm, the F-P bottle was purged 15 times with H_2 (5 s per purge), filled with 2.7 atm of H_2 , and then $t = 0$ was set via the PC interface. Ten repeats of this Standard Conditions experiments were performed yielding the same plot shown in Figure 1 with the initial rates within $\pm 5\%$.

When the hydrogen uptake ceased, as monitored via the PC interfaced pressure transducer, the F-P bottle was disconnected from the hydrogenation line, the remaining H_2 pressure was released, and the F-P bottle was transferred back into the drybox. There, a disposable plastic pipet was used to withdraw a ~ 0.1 mL aliquot from the culture tube, which was then mixed with 1 mL of CD_2Cl_2 in an individual glass ampule and then transferred into an NMR sample tube. The NMR tube was sealed and brought out of the drybox for 1H NMR examination to confirm that all the observed H_2 pressure loss had gone into the cyclohexene-to-cyclohexane reduction reaction.

The above detailed procedure was also followed for 62 °C, 3.4 atm initial H_2 pressure cyclohexene hydrogenation investigation with one change: after following the same preparation procedure in the drybox, the sealed F-P bottle was removed from the drybox, placed into a constant temperature circulating bath at 62 °C, and stirred (at 600 rpm) for 10 min so that the reaction solution reached the desired reaction temperature, 62 °C, at which point 3.4 atm H_2 pressure was applied.

Second, Subsequent Cyclohexene Hydrogenations. For the subsequent cyclohexene hydrogenation, the above “standard conditions cyclohexene hydrogenation ...” procedure was repeated. When the hydrogen uptake ceased, again as monitored via the PC interfaced pressure transducer, and in separate 22 and 62 °C cyclohexene hydrogenation reactions, *vide supra*, the F-P bottle was disconnected from the hydrogenation line, the remaining H_2 pressure was released, and the F-P bottle was transferred back into the drybox. There, 1.0 mL of fresh cyclohexene was added to the culture tube in the F-P bottle for a second, subsequent cyclohexene hydrogenation with the catalyst formed during the first hydrogenation, again in separate experiments at 22 and 62 °C. Then the F-P bottle was sealed, removed from the drybox, placed into a constant temperature circulating bath at 22 °C, and then attached via Swagelok TFE-sealed Quick-Connects to the hydrogenation line (which had already been evacuated >30 min to remove any possible trace amount of O_2 and H_2O) and refilled with 2.7 atm of purified H_2 . Stirring was started at 600 rpm, the F-P bottle was purged 15 times with H_2 (5 s per purge) and filled with 2.7 atm of H_2 , and $t = 0$ was set on the PC interface. Three repeats of this second, subsequent cyclohexene hydrogenation at 22 °C were performed, yielding the same initial rates within $\pm 5\%$ experimental error (Figure S1, Supporting Information).

Similarly, two repeats of the second, subsequent cyclohexene hydrogenation at 22 °C were performed and yielded the same initial rates within $\pm 5\%$ experimental error.

UV–Vis Investigation of the Cyclohexene Hydrogenation Product Solutions and $[\text{RhCp}^*\text{Cl}_2]_2$. When the hydrogen uptake ceased (as monitored via the PC interfaced pressure transducer) for separate cyclohexene hydrogenation reactions beginning with $[\text{RhCp}^*\text{Cl}_2]_2$ at 22, 26, or 62 °C and respective initial H_2 pressures of 2.7, 3.4, and 3.4 atm, the F-P bottle was disconnected from the hydrogenation line, the remaining H_2 pressure was released, and the F-P bottle was transferred back into the drybox. There, 0.5 mL of the product solution was filtered through a 0.2 μm Nalgene nylon filter and diluted to 5 mL with fresh 2-propanol in a 20 mL scintillation glass vial. Next, the filtered solution was transferred into an O_2 -free quartz UV–vis cuvette, sealed, and removed from the drybox for UV–vis investigation. The resultant $[\text{Rh}]_{\text{total}}$ equals 5.2×10^{-4} M for each of these three different temperature and pressure cyclohexene hydrogenation reactions.

A UV–vis reference spectrum of the $[\text{RhCp}^*\text{Cl}_2]_2$ starting material was prepared as follows: In the drybox, 8.0 mg of $[\text{RhCp}^*\text{Cl}_2]_2$ was weighed in a 20 mL scintillation glass vial into which a new $5/8 \times 5/16$ in. Teflon-coated stir bar was then also placed. Next, 4.5 mL of 2-propanol, 0.5 mL of cyclohexene, and 0.05 mL of triethylamine were added in separate gastight syringes, and the resulting solution was stirred ~ 30 min, yielding a clear, orange-red solution, then this clear, orange-red solution was transferred into an O_2 -free quartz UV–vis cuvette, sealed, and removed from the drybox for UV–vis investigation. This procedure yielded the same total rhodium concentration, $[\text{Rh}]_{\text{total}} = 5.2 \times 10^{-4}$ M, as in the case of cyclohexene hydrogenation product solutions, *vide supra*.

Calculation of the Initial Rate. Initial rates were calculated from the cyclohexene concentration (M) vs time (h) data by drawing a tangent to the initial portion of the kinetic data, as shown, for example, in Figure 1. Then the slope of this tangent line was calculated using $y = -mx + b$ and Microsoft Excel, resulting in the initial rate, $-m$. The initial rates for all the second, subsequent cyclohexene hydrogenations were corrected for the changed volumes, 10 (first run)–11 mL (second run,) by multiplying the initial rate observed in the second run by $11/10 = 1.1$.

1,10-Phenanthroline Kinetic Quantitative Poisoning Experiments. For each 1,10-phenanthroline quantitative poisoning experiment, a standard conditions cyclohexene hydrogenation beginning with $[\text{RhCp}^*\text{Cl}_2]_2$ at 22 °C and 2.7 atm initial H_2 pressure was started. When the reaction was completed, as judged by the cessation of H_2 pressure loss and confirmation of the cyclohexane product by ^1H NMR, the F-P bottle was disconnected from the hydrogenation line, the remaining H_2 pressure was released, and the F-P bottle was transferred back into the drybox. There, 1.0 mL of fresh cyclohexene plus a quantitative, predetermined amount of 1,10-phenanthroline were added to the solution in a series of five separate experiments, specifically: 0.1, 0.3, 0.5, 0.7, and 1.0 equiv of 1,10-phenanthroline per total equivalents Rh present (0.0052, 0.016, 0.026, 0.036, and 0.052 mmol or 0.9, 2.8, 4.7, 6.6, and 9.4 mg, respectively). Then, for each individual experiment, the F-P bottle was sealed, removed from the drybox, placed into a constant temperature circulating bath at 22 °C, attached via Swagelok TFE-sealed Quick-Connects to the hydrogenation line (which had already been evacuated >30 min to remove any possible trace amount of O_2 and H_2O), and refilled with 2.7 atm of purified H_2 . Stirring was started at 600 rpm, the F-P bottle was purged 15 times with H_2 (5 s per purge) and filled with 2.7 atm of H_2 , and $t = 0$ was set via the

PC interface. See the [Supporting Information](#) for the plots of the resultant hydrogenation data and the corresponding initial rates for each poisoning experiment. Each 1,10-phenanthroline quantitative poisoning experiment was repeated two times and yielded reproducible initial rates within $\pm 10\%$.

The same procedure was followed for the 62 °C, 3.4 atm initial H_2 pressure cyclohexene hydrogenation product solution (*vide infra*; see the [Results and Discussion](#)) of predominantly Rh_4 clusters. Briefly, 1.0 mL of fresh cyclohexene plus a quantitative, predetermined amount of 1,10-phenanthroline were added (in the drybox, as detailed above) to the product solution of 62 °C, 3.4 atm initial H_2 pressure cyclohexene hydrogenation reaction beginning with $[\text{RhCp}^*\text{Cl}_2]_2$ in a series of three separate experiments, specifically 0.1, 0.3, and 0.5 equiv of 1,10-phenanthroline per total equiv of Rh present (0.0052, 0.016, and 0.026 mmol or 0.9, 2.8, and 4.7 mg, respectively). Then for each individual experiment, the F-P bottle was sealed, removed from the drybox, placed into a constant-temperature circulating bath at 22 °C, and attached via Swagelok TFE-sealed Quick-Connects to the hydrogenation line (which had already been evacuated >30 min to remove any possible trace amount of O_2 and H_2O) and refilled with 2.7 atm of purified H_2 . Stirring was started at 600 rpm, the F-P bottle was purged 15 times with H_2 (5 s per purge) and filled with 2.7 atm of H_2 , and $t = 0$ was set via the PC interface. See the [Supporting Information](#) for the plots of the resultant hydrogenation data and the corresponding initial rates for each poisoning experiment. Each 1,10-phenanthroline quantitative poisoning experiment was repeated two times and yielded reproducible initial rates within a $\pm 10\%$ experimental error.

Qualitative Hg(0) Poisoning Experiment. A standard conditions cyclohexene hydrogenation beginning with $[\text{RhCp}^*\text{Cl}_2]_2$ at 22 °C and 2.7 atm initial H_2 pressure was started. When the reaction was completed (as judged by the cessation of H_2 pressure loss and the cyclohexane product confirmed by ^1H NMR), the F-P bottle was disconnected from the hydrogenation line, the remaining H_2 pressure was released, and the F-P bottle was transferred back into the drybox. There, 1.0 mL of fresh cyclohexene plus ~ 300 equiv of Hg(0) per total equivalents of Rh (~ 1.7 g) were added to the solution, then the F-P bottle was sealed, removed from the drybox, placed into a constant temperature circulating bath at 22 °C, attached via Swagelok TFE-sealed Quick-Connects to the hydrogenation line (which had already been evacuated >30 min to remove any possible trace amount of O_2 and H_2O), and refilled with 2.7 atm of purified H_2 . A Fauske and Associates Super Magnetic Stirrer plate was utilized for stirring with a variable speed control knob and an LED display showing the stirring rate. Stirring was started at 600 rpm, the F-P bottle was purged 15 times with H_2 (5 s per purge) and filled with 2.7 atm of H_2 , and $t = 0$ was set via the PC interface. After ~ 1.5 h, the stirring speed was increased to 1000 rpm, and the reaction was followed for an additional 8.5 h. The same procedure was repeated two times, yielding the same initial rate within a $\pm 10\%$ experimental error.

The same procedure was followed for the 62 °C, 3.4 atm initial H_2 pressure cyclohexene hydrogenation product solution (*vide infra*; see the [Results and Discussion](#)) of predominantly Rh_4 clusters. Briefly, 1.0 mL of fresh cyclohexene plus ~ 300 equiv of Hg(0) per total equivalents of Rh (~ 1.7 g) were added (in the drybox, as detailed above) to the product solution of 62 °C, 3.4 atm initial H_2 pressure cyclohexene hydrogenation reaction. The F-P bottle was then sealed, removed from the

drybox, placed into a constant-temperature circulating bath at 22 °C, and attached via Swagelok TFE-sealed Quick-Connects to the hydrogenation line (which had already been evacuated >30 min to remove any possible trace amount of O₂ and H₂O and refilled with 2.7 atm of purified H₂). Stirring was started at 1000 rpm, the F-P bottle was purged 15 times with H₂ (5 s per purge) and filled with 2.7 atm of H₂, and $t = 0$ was set via the PC interface. This Hg(0) poisoning experiment was repeated two times; both experiments produced complete poisoning of the extant catalyst.

In Operando XAFS and ¹H NMR Investigations. *Materials and Instrumentation.* Data analysis and fit methods were followed as detailed previously.^{6,19} The rhodium K-edge (23,222 eV) XAFS spectra were collected in a stirred, stainless steel reactor with PEEK windows⁶ in transmission mode on the bending magnet beamline (PNC-CAT, Sector 20) at the Advanced Photon Source, Argonne National Laboratory. No evidence of beam-created photoelectron or other damage was observed during exposure of the rhodium complexes to the X-rays. Details of the XAFS beamline are given elsewhere.¹⁹ Portions of Athena and Artemis programs were used for the analysis of the XAFS data with theoretical standards calculated using FEFF8.²⁰ The XAFS $\chi(k)$ data were weighted by k^3 and windowed between $2.0 < k < 19.0 \text{ \AA}^{-1}$ using a Hanning window with $dk = 1.0 \text{ \AA}^{-1}$.

In Operando XAFS Studies. These were performed identically to those in our recent, detailed report,⁶ with the same pressure cell described in detail therein. The experimental procedure is briefly described here. In all XAFS experiments, the reactor was loaded under a nitrogen or helium atmosphere in a glovebox and sealed, and the atmosphere was replaced by three pressurizations of H₂ to 8.7 atm. The cell was then placed in the XAFS beam, and the spectra were collected. The temperature was monitored, and a new cell was used for each experiment to avoid the possibility of contamination from a previous run interfering with the results.

In Operando ¹H NMR Studies. In the glovebox, 5 ± 1 mg of [RhCp*Cl₂]₂ (0.007 mmol) was weighed into a 2-dram glass vial, and 0.80 mL of perdeuterated 2-propanol (Cambridge Isotopes, used as received), 0.01 mL of cyclohexene (0.099 mmol), and 0.11 mL of perdeuterated triethylamine (Cambridge Isotopes, used as received) (0.077 mmol) were added via separate gastight syringes. The relative amount of cyclohexene is much lower in the NMR experiment than in the kinetic experiments to keep the proton NMR signals on scale. Hence, the ratio of cyclohexene to rhodium is much lower in this NMR experiment. After mixing, 0.30 mL of this solution was syringed into a PEEK high-pressure NMR cell.²¹ The cell was sealed, brought out of the box, and attached to a gas manifold system. The headspace in the PEEK cell was removed and replaced by a constant pressure of 2.7 atm dried H₂ gas via a syringe pump. Between spectral collections, the gas–liquid contents in the PEEK cell were mixed via a vortex mixer. Proton NMR readings were collected at 500 MHz on a Varian spectrometer using a 13° pulse, 5 s acquisition time, and a 1 s recycle time. Spectra were referenced internally to the residual protio-fraction of the deuterated solvent.

RESULTS AND DISCUSSION

Controls of a Standard Conditions Cyclohexene Hydrogenation Beginning with [RhCp*Cl₂]₂ at 22 °C and 2.7 atm Initial H₂ Pressure. A standard conditions cyclohexene hydrogenation beginning with [RhCp*Cl₂]₂ at 22

°C and 2.7 atm initial H₂ pressure was performed as a control to check the reproducibility of the system in one of our (E.B.'s) hands, following the previously reported procedure¹⁰ also detailed in the **Experimental** section herein. As previously seen,¹⁰ (i) the cyclohexene hydrogenation reaction started immediately (Figure 1) without a detectable induction period and took ~4.5 h to go to completion, reproducing our previous report.¹⁰ The initial rate of the reaction as shown in Figure 1 is $-\{d[\text{cyclohexene}]/dt\}_{\text{initial}} = 0.61 \pm 0.05 \text{ M/h}$. When the H₂ uptake ceased after ~4.5 h, (ii) the solution had changed from its initial orange-red to dark red, and (iii) the hydrogenation of cyclohexene to cyclohexane was complete (as verified by both the cessation of pressure loss and by ¹H NMR, the latter confirming that all the cyclohexene had been consumed and a concomitant, stoichiometric amount of cyclohexane had been formed). In addition, (iv) there was no visually observable metal precipitate. Each of (i–iv) is consistent with our previous report¹⁰ and demonstrates the reproducibility of the system in our hands.

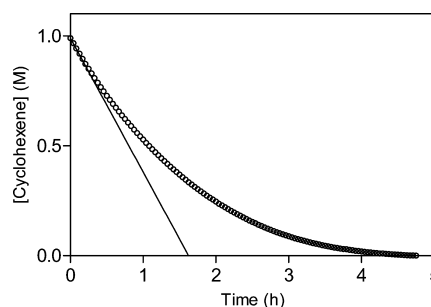


Figure 1. A standard conditions cyclohexene hydrogenation curve beginning with [RhCp*Cl₂]₂ at 22 °C and 2.7 atm initial H₂ pressure. The cyclohexene hydrogenation activity starts immediately with an initial rate of $-\{d[\text{cyclohexene}]/dt\}_{\text{initial}} = 0.61 \pm 0.05 \text{ M/h}$, according to the indicated tangent to the initial portion of the data. The total reaction time is ~4.5 h.

A Second, Subsequent Cyclohexene Hydrogenation with the Evolved Catalyst Solution.

A subsequent cyclohexene hydrogenation reaction was performed with the evolved catalyst produced during the first run, as detailed in the **Experimental** section. See the Supporting Information for the hydrogenation curve (Figure S1). The initial rate of the subsequent cyclohexene hydrogenation (corrected for the now 11 vs prior 10 mL of solution, as detailed in the **Experimental** section) is $-\{d[\text{cyclohexene}]/dt\}_{\text{initial}} = 0.55 \pm 0.05 \text{ M/h}$, that is, the same as the first run ($0.61 \pm 0.05 \text{ M/h}$) within $\pm 10\%$.

However, the kinetics in this second run are clearly biphasic, that is, contain two distinct “phases” or components in time and cannot be fit by, for example, a single exponential phase (see Figure S1); those kinetics, plus the 20 h reaction time (vs 4.5 h for the first run in Figure 1), suggest that some catalyst deactivation is occurring, resulting in the second, slower kinetic phase.²² The color of the solution at the end of the subsequent cyclohexene hydrogenation run is, however, still dark red, and the filtered solution exhibits a decreased intensity version of the UV–vis spectrum as the first run (Figure S2). Hence, the filtering does remove some insoluble, presumably deactivated catalyst material that has been formed. See the **Supporting Information** if further details are desired about either the biphasic kinetics or the catalyst deactivation process.

Overall, the first and the subsequent second cyclohexene hydrogenation data reproduce our previous report;¹⁰ specifically, (i) the cyclohexene hydrogenation starts immediately without any detectable induction period; and (ii) a dark-red solution is produced upon the complete hydrogenation of cyclohexene to cyclohexane as confirmed by ¹H NMR. In addition, (iii) the initial rate, $-\{d[\text{cyclohexene}]/dt\}_{\text{initial}}$ of the first and the subsequent cyclohexene hydrogenation reactions are the same within $\pm 10\%$ experimental error; but (iv) non-first-order, biphasic kinetics and a longer 20 h (vs 4.5 h in Figure 1) reaction completion time are seen in the second, subsequent cyclohexene hydrogenation curve, a result that suggests that detectable catalyst deactivation is occurring in the second, subsequent hydrogenation run.

Initial In Operando XAFS Investigation at 26 °C and 8.3 atm Initial H₂ Pressure Revealing the Formation of Rh₄ Clusters. The XAFS studies that follow were necessarily performed at 4-times higher rhodium concentrations, needed to attain sufficient signal-to-noise in the XAFS, as compared with the standard reaction conditions concentration used for the kinetics. Figure 2 shows the real and imaginary parts of the

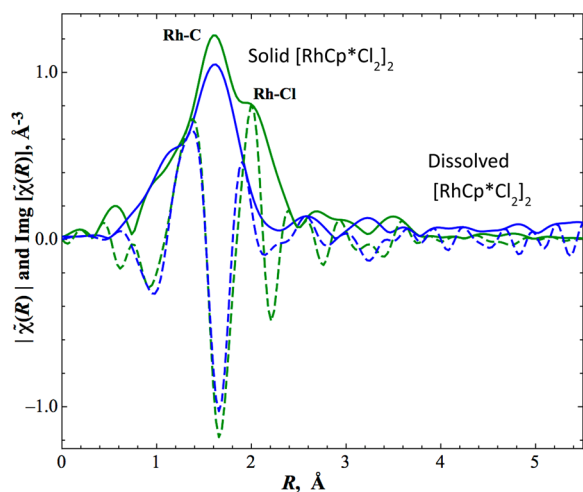


Figure 2. k^2 -Weighted $|\tilde{\chi}(R)|$ (solid lines) and $\text{Im}[\tilde{\chi}(R)]$ (dashed lines) plots for the solid $[\text{RhCp}^*\text{Cl}_2]_2$ (green) and that freshly dissolved in 2-propanol with triethylamine and cyclohexene prior to addition of H_2 at 26 °C (blue). Note the loss of (i) Rh–Cl scattering at 1.9 Å and, although it is less definitive, the apparent loss of (ii) Rh–Rh scattering at 3.6 Å upon dissolving solid $[\text{RhCp}^*\text{Cl}_2]_2$ in 2-propanol, triethylamine, and cyclohexene (and without H_2). In all cases, the k range for the Fourier transform is 2–14 Å⁻¹. Distances are not corrected for photoelectron phase shifts.

Fourier transform of the EXAFS of crystalline solid $[\text{RhCp}^*\text{Cl}_2]_2$ and $[\text{RhCp}^*\text{Cl}_2]_2$ dissolved in the reaction solvent (triethylamine, 2-propanol, and cyclohexene), to start without H_2 pressure. This Figure demonstrates unequivocally that simply dissolving $[\text{RhCp}^*\text{Cl}_2]_2$ in the reaction solvent changes the structure of the rhodium complex. Visual inspection of Figure 2 shows the loss of some rhodium chloride scattering (shown as shoulder-centered at 1.9 Å in the spectrum of the solid) and the loss of some rhodium-to-rhodium scattering at 3.6 Å, which is consistent with the initial rhodium dimer being cleaved at least partially into rhodium-containing monomers. It is difficult to determine if solvent molecules have replaced the initial chlorides because the small solvent atoms (C, N, or O) would scatter the X-rays similar to,

and overlap with, those of the carbons from the Cp^* ligand. However, fitting the XAFS spectra with FEEF8 (Figure S3, Table S1) is consistent with ~50% of the initial dimer being intact and the remainder of the rhodium species being a monomer of unknown composition, with the crucial result being that ~50% of the initial $[\text{Cp}^*\text{Rh}]_2$ dimer has been converted to a monomeric, Cp^*Rh_1 species.

Upon the addition of H_2 gas, the monomer begins to transform into Rh_4 clusters at a slow rate. Two hours after the cyclohexene has been reduced to cyclohexane, the XAFS spectrum appears to stop transforming into the Rh_4 complex. Comparison of the XAFS results with cyclohexene with those at 100 °C with benzene⁶ (Figures S4, S5) shows that not all of the rhodium is in the form of Rh_4 clusters. XAFS spectra, collected long after the cyclohexene reduction reaction was complete, show no change in the rhodium complexes' structure (Figure S3). This, in turn, indicates that under the milder conditions of 26 °C and 8.3 atm initial H_2 pressure, no reduction of the cyclopentadiene ligand has occurred (i.e., and in contrast to the higher temperatures of benzene hydrogenation,⁶ at which the hydrogenation of cyclopentadiene is evident).

Finally, and as already noted earlier, we emphasize that by “ Rh_4 ” clusters we do not mean to imply “naked” Rh_4 clusters. Instead and as before,⁶ ligands are, of course, present on these clusters, notably the $\text{Rh}_4\text{Cp}^*_4\text{H}_3^+$ detected (vide infra) by ex situ MS in these 22 °C studies, or, as in the average composition of “ $\text{Rh}_4\text{Cp}^*_{2.4}\text{Cl}_4\text{H}_c$ ”, identified previously⁶ at 100 °C.

In summary of the in operando XAFS, the results clearly show the loss of Rh–Cl in the initial dimer $[\text{RhCp}^*\text{Cl}_2]_2$ simply upon dissolution in the 2-propanol reaction solvent with triethylamine and without the addition of H_2 . The results also show that the starting $[\text{RhCp}^*\text{Cl}_2]_2$ is slowly transformed into (ligated) Rh_4 clusters,²³ similar to what is observed at higher, 100 °C temperatures and 50 atm pressures during benzene hydrogenation.⁶ The key point for the present studies, then, is that detectable amounts of this starting dimeric Rh_2 , some Rh_1 , as well as Rh_4 species exist during cyclohexene hydrogenation catalysis. Hence, each of these species, as well as trace, undetected, but conceivably highly active $\text{Rh}(0)_n$ nanoparticles, are viable hypotheses for the kinetically dominant, true catalyst.

In Operando ¹H NMR Investigations. A standard conditions cyclohexene hydrogenation beginning with $[\text{RhCp}^*\text{Cl}_2]_2$ at 22 °C and 2.7 atm constant H_2 pressure was followed via in operando ¹H NMR in a PEEK high-pressure NMR tube, as detailed in the Experimental section. The Cp^* hydrogen resonance at 1.55 ppm of $[\text{RhCp}^*\text{Cl}_2]_2$ dissolved in CD_2Cl_2 was found to be significantly different, 1.86 ppm, from when dissolved in the reaction solvent mixture of 2-propanol, triethylamine, and cyclohexene (Figure S6) in the ¹H NMR. During the reaction, the Cp^* resonance did not change from 1.86 ppm; neither did any new resonances that could be identified as being from new Cp^* -containing complexes (Figures S7 and S8), nor were the resonances for hydrogenated Cp^* products observed. Specifically, none of the previously observed $\text{Cp}^*\text{-H}_3$ and $\text{Cp}^*\text{-H}_5$ formed during benzene hydrogenation at higher pressures and temperatures were seen⁶ (Figure S8 of the Supporting Information). A search was also made for possible hydride signals, as expected for the $[\text{RhCp}^*(\text{H})_2(\text{solvent})]$ catalyst proposed by Maitlis,⁹ but only one very weak hydride signal at ~ -11.3 ppm was detected, which integrated to just ~ 0.2 hydrogens (vs the 15 hydrogens of Cp^*). As expected for a reactive intermediate, the hydride

appears only during the middle of the reaction and is not observable after all of the cyclohexene has been hydrogenated to cyclohexane.

The proton NMR results confirm the XAFS by indicating a change in the structure of $[\text{RhCp}^*\text{Cl}_2]_2$ when dissolved in the reaction solvent 2-propanol plus triethylamine, resulting in the observation of a single Cp^* resonance (Figure S8). The ^1H NMR results also imply the formation of a $\text{Rh}-\text{H}$ and indicate that no new, detectable Cp^* resonances appear during the reaction.

Ex Situ MS and UV–Vis Verification of the Formation of Rh_4 Clusters. To see if we could verify the XAFS detection of Rh_4 by a second, “in-house” method, a cyclohexene hydrogenation was performed at the maximum pressure possible with the pressure transducer on the hydrogenation line, 3.4 atm, and also at 26 °C to come as close to the XAFS conditions (8.3 atm; 26 °C) as possible. The catalytic activity in the 3.4 atm, 26 °C run again started immediately with no detectable induction period ($-\{d[\text{cyclohexene}]/dt\}_{\text{initial}} = 0.76 \pm 0.05 \text{ M/h}$ (Figure S9 of the Supporting Information). The resulting final solution was green, diagnostic of the formation of Rh_4 clusters.^{6,24} MS analysis of the green product solution confirmed the presence of ligated Rh_4 clusters via a $m/z = 955$ signal that matches precisely the expected isotope distribution of $[\text{Rh}_4\text{Cp}^*_4\text{H}_3]^+$ (see the Supporting Information, Figure S10). The formation of the green product was confirmed in three repeat experiments at the 3.4 atm and at 26 °C conditions.

What is striking is that the small change to a slightly higher temperature and pressure, over a standard conditions hydrogenation (2.7 atm and 22 °C), leads to the observation of a green, Rh_4 -containing solution. This led us to check for the presence of any MS-detectable $[\text{Rh}_4\text{Cp}^*_4\text{H}_3]^+$ in a standard conditions, 22 °C and 2.7 atm H_2 initial pressure, cyclohexene hydrogenation reaction beginning with $[\text{RhCp}^*\text{Cl}_2]_2$. The resultant dark-red product solution showed no detectable $m/z = 955$ peak indicative of $[\text{Rh}_4\text{Cp}^*_4\text{H}_3]^+$, nor any other Rh_4 cluster in combination with any of the available ligands present: Cp^* , Cl , or H (Figure S11 of the Supporting Information).

Of further interest here is that the dark-red product solution turns green when concentrated (i.e., the product solution of a standard conditions cyclohexene hydrogenation reaction). Specifically, while 10 mL of dark-red product solution was being vacuum-dried in the drybox, the color of the solution became green once $\sim 1\text{--}2$ mL of solution remains, an experiment that was repeated twice with identical results. In short, green Rh_4 cluster formation is sensitive to concentration, H_2 pressure and temperature, higher values in each variable generally favoring formation of the Rh_4 cluster.

Ex Situ UV–Vis Investigation. UV–vis analyses of the dark-red solution and also of the green product solution (produced at 26 °C and 3.4 atm H_2 pressure) were obtained as detailed in the Experimental section. The spectra shown in Figure 3 reveal two absorption bands for the dark-red product, 466 and 528 nm, but only one main absorption band for the green product: 638 nm. These spectra and main bands are not only sufficiently distinct from each other, but are also distinct from those for the precatalyst, $[\text{RhCp}^*\text{Cl}_2]_2$. Importantly, within the detection limits of UV–vis, it is inferred that the dark-red solution is predominantly Rh_1 and the green solution is predominantly Rh_4 , the latter being consistent with the in operando XAFS and ex situ MS investigations (vide supra).

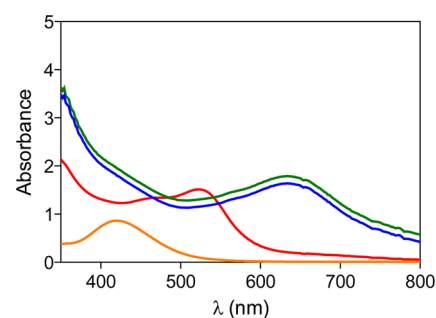


Figure 3. UV–visible spectra of the cyclohexene hydrogenation product solutions in an O_2 -free quartz UV–vis cuvette at 22 °C under N_2 and for the 2.7 atm H_2 pressure product (red line); for the 26 °C, 3.4 atm H_2 pressure product (blue line); and for the 62 °C, 3.4 atm H_2 pressure product (green line), all beginning with $[\text{RhCp}^*\text{Cl}_2]_2$. All product solutions were diluted with 2-propanol to yield a $[\text{Rh}]_{\text{total}}$ of $5.2 \times 10^{-4} \text{ M}$, as detailed in the Experimental section. For comparison, the spectra of the $[\text{RhCp}^*\text{Cl}_2]_2$ is also shown (orange line) with the same total Rh concentration, a $[\text{Rh}]_{\text{total}}$ of $5.2 \times 10^{-4} \text{ M}$. The blue and green spectra are characteristic of Rh_4 , and the red is assigned to a Rh_1Cp^* species, as discussed more in the main text.

Important conclusions from the ex-situ UV–visible and MS experiments are that they (i) do detect Rh_4 clusters under selected conditions and, therefore and thereby, are supportive of the more direct, compelling detection of Rh_4 clusters in operando by XAFS and that they (ii) do show a Rh product distinctly different from the $[\text{RhCp}^*\text{Cl}_2]_2$ starting material.

The additional confirmation of the presence of Rh_4 clusters raises the alternative hypothesis that trace Rh_4 clusters could still well be the dominant cyclohexene hydrogenation catalyst at the 22 °C and 2.7 atm H_2 pressure conditions utilized herein. Hence, quantitative kinetic poisoning studies were investigated next to provide insights into the true 22 °C, 2.7 atm initial H_2 pressure hydrogenation catalyst when beginning with $[\text{RhCp}^*\text{Cl}_2]_2$. Indeed, the present studies are analogous to our past studies in which quantitative poisoning studies proved crucial in providing compelling evidence for the true catalyst.⁶

Quantitative 1,10-Phenanthroline Kinetic Poisoning Experiments. Quantitative 1,10-phenanthroline kinetic poisoning experiments were performed with the catalyst produced by a first cyclohexene hydrogenation run.²⁵ As detailed in the Experimental section, in the drybox in a series of five separate experiments, a predetermined amount of 1,10-phenanthroline was dissolved in 1.0 mL of fresh cyclohexene (specifically 0.1, 0.3, 0.5, 0.7, and 1.0 equiv of 1,10-phenanthroline per total Rh) and then added to the product solution from a first run of cyclohexene hydrogenation performed under standard conditions. The initial rates were then computed for each of these five separate 1,10-phenanthroline poisoning experiments, and then each of those initial rates was then divided by the initial rate without any 1,10-phenanthroline present (i.e., by $-\{d[\text{cyclohexene}]/dt\}_{\text{initial}} = 0.55 \pm 0.05 \text{ M/h}$; Figure S12) and used to construct the poisoning plot shown in Figure 4.

The increased equivalents of 1,10-phenanthroline gradually slowed down the catalytic reaction and 1.0 equiv of 1,10-phenanthroline per total rhodium poisoned the catalyst completely (Figure 4). The key result from Figure 4 is that ~ 1.0 equiv of 1,10-phenanthroline poison per total rhodium present completely deactivates and poisons the catalyst, consistent with and supportive of a Rh_1Cp^* -based catalyst.

MS Identification of a Poisoned, $[\text{Rh}_1\text{Cp}^*\text{Cl}(1,10\text{-phenanthroline})]^+$ Adduct. Significantly, MS analysis of the

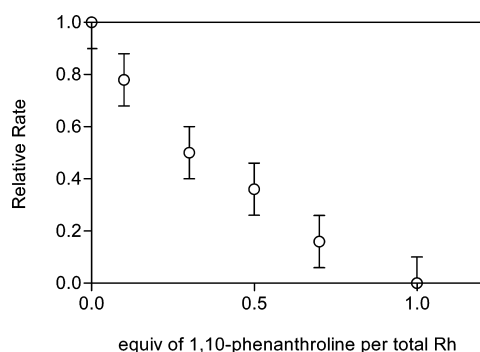


Figure 4. Plot of the relative rate vs equivalents of 1,10-phenanthroline per total Rh present. The results demonstrate that the addition of 1.0 equiv of 1,10-phenanthroline per total Rh present poisons the catalyst completely, results that are consistent with a single metal, Rh_1Cp^* -based catalyst with, apparently, up to two available coordination sites per Rh for the 1,10-phenanthroline poison.

product solutions of all five of the separate quantitative 1,10-phenanthroline poisoning experiments reveal a $m/z = 453$ peak that matches precisely the theoretical isotope distribution expected for $[\text{Rh}_1\text{Cp}^*\text{Cl}(1,10\text{-phenanthroline})]^+$ (Figure 5). Moreover, no signal attributable to a 1,10-phenanthroline-poisoned Rh_4 cluster catalyst could be detected (i.e., no peak that matched any combination of Rh_4 with the other possible ligands present: Cp^* , Cl, H, and 1,10-phenanthroline). This constitutes a relatively rare example in which the poisoned catalyst has been detected as part of studies focused on determining the true active catalyst.^{1,12} The poisoning data in Figure 4, when combined with the detection of the $[\text{Rh}_1\text{Cp}^*\text{Cl}(1,10\text{-phenanthroline})]^+$ as the poisoned product, add considerable credence to the hypothesis of a Rh_1Cp^* -based species as the dominant catalyst in the 22 °C and 2.7 atm initial H_2 pressure cyclohexene hydrogenation system investigated herein.

Activity and Poisoning Controls of the Evolved Rh_4 Clusters Formed at 62 °C and 3.4 atm Initial H_2 Pressure Then Studied at 22 °C and 2.7 atm Initial H_2 Pressure.

Next, a sample of predominantly Rh_4 clusters was prepared as detailed in the Experimental section via the 62 °C and 3.4 atm H_2 pressure cyclohexene hydrogenation beginning with $[\text{RhCp}^*\text{Cl}_2]_2$ (Figure S13). The resultant Rh_4 clusters were used in quantitative 1,10-phenanthroline poisoning experiments, but now, of course, at 22 °C and 2.7 atm H_2 pressure. The first results of interest here are (i) that catalytic cyclohexene hydrogenation at 22 °C and 2.7 atm H_2 begins immediately and smoothly, without any detectable induction period, at an initial rate of $-\{d[\text{cyclohexene}]/dt\}_{\text{initial}} = 0.35 \pm 0.05$ M/h (see the Supporting Information, Figure S14); (ii) the product solution post the cyclohexene hydrogenation remained green and showed the identical UV–vis spectrum (i.e., as in Figure 3) as seen for the preformed Rh_4 clusters; and (iii) a MS signal at $m/z = 955$ characteristic of $[\text{Rh}_4\text{Cp}^*_4\text{H}_3]^+$ was also observed for the green product solution, as expected (Figure S15). The green Rh_4 clusters appear to be relatively stable under the reaction conditions and in particular do not fragment back into dark-red Rh_1 species (by both UV–vis and MS evidence).

Next, 1,10-phenanthroline poisoning experiments were performed by increasing the equivalents of 1,10-phenanthroline per total rhodium gradually (Figure S16) until the catalyst was poisoned completely (Figure 6). The results show that (i) the addition of 0.5 equiv of 1,10-phenanthroline per total Rh present poisons the catalyst completely. In addition, (ii) the nearly linear form of the plot indicates strong, irreversible 1,10-phenanthroline bindings⁸ to Rh_4 clusters at 22 °C. Worth noting here is that at 100 °C, the Rh_4 clusters also required 0.5 equiv of 1,10-phenanthroline per total Rh to be poisoned (in that work, 2 equiv of 1,10-phenanthroline per total Rh_4 cluster, a ratio of 0.5), results that pleasingly match the present 22 °C results (and even though a somewhat sigmoidal 1,10-phenanthroline quantitative poisoning curve is seen⁶ at 100 °C, which had to be analyzed via a weaker, reversible binding poison kinetic model⁸).

Analysis of the product solution from the 0.5 equiv of 1,10-phenanthroline poisoning experiment by MS did not reveal any signal that could be attributed to 1,10-phenanthroline bound to

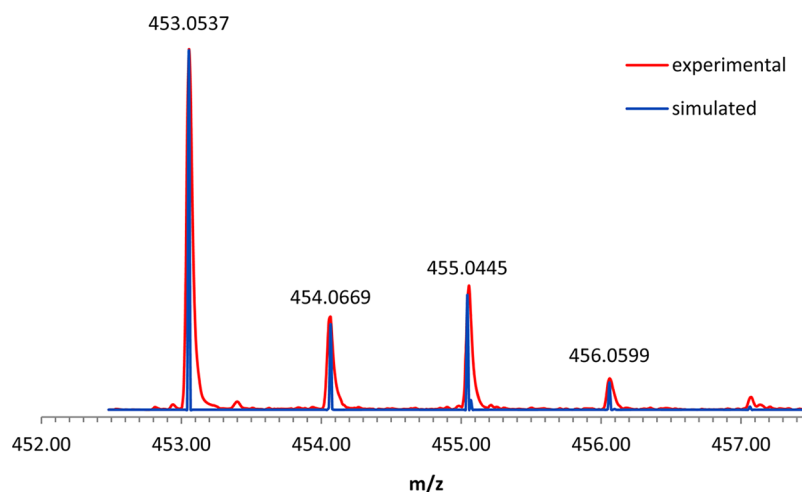


Figure 5. A MS spectrum of the product solution of quantitative 1,10-phenanthroline poisoning experiment for 1.0 equiv of 1,10-phenanthroline per total rhodium in comparison with the superimposed theoretical values calculated for $[\text{Rh}_1\text{Cp}^*\text{Cl}(1,10\text{-phenanthroline})]^+$. The same $m/z = 453$ signal with the same isotope distribution was observed for all five of the separate quantitative 1,10-phenanthroline poisoning experiments. The observed isotope distribution matches the theoretical values exactly: observed: m/z 453 (M^+ , 100%), 454 (30%), 455 (35%), 456 (9%), 457 (1%); theoretical: m/z 453 (M^+ , 100%), 454 (30%), 455 (35%), 456 (9%), 457 (1%).

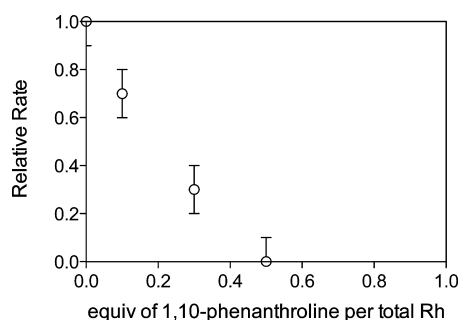


Figure 6. Plot of the relative rate vs equivalents of 1,10-phenanthroline per total Rh present for the ostensibly Rh_4 -based catalyst. The results demonstrate that increased equivalents of 1,10-phenanthroline poison the catalytic activity, and that the addition of 0.5 equiv of 1,10-phenanthroline per total Rh present poisons the catalyst completely.

a Rh_4 cluster. However, neither was a $m/z = 453$ signal for $[\text{RhCp}^*\text{Cl}(1,10\text{-phenanthroline})]^+$ detected, (negative) evidence consistent with the previously stated lack of fragmentation of Rh_4 clusters to Rh_1 species (vide supra), either in solution or under the MS analysis conditions.

Significantly, the 1,10-phenanthroline quantitative poisoning experiments reveal that one can differentiate a homogeneous Rh_1Cp^* -based catalyst from a Rh_4 subnanometer cluster-based homogeneous catalyst by their requirement for 1.0 vs 0.5 equiv of 1,10-phenanthroline per total rhodium present for their respective complete poisoning under otherwise identical reaction conditions. Overall, the 1,10-phenanthroline quantitative kinetic poisoning experiments are consistent with and highly supportive of a homogeneous Rh_1Cp^* -based species as the true cyclohexene hydrogenation catalyst derived from $[\text{RhCp}^*\text{Cl}_2]_2$ under the 22 °C, 2.7 atm H_2 pressure and other specific standard reaction conditions employed herein.

We can furthermore understand why Rh_4 is not the kinetically dominant catalyst under the present conditions: Figures 1 and S14 show that, per Rh present, the catalytic activity for cyclohexene hydrogenation under standard conditions employed herein of Rh_1Cp^* vs Rh_4 is $\sim 0.61/0.35$ or 1.7. That is, the Rh_1Cp^* -based catalyst is only 1.7-fold more active than Rh_4 per Rh present so that a main reason Rh_1Cp^* is the kinetically dominant catalyst is because it is also the dominant form of the Rh mass present under the reaction conditions.

Testing and Ruling Out the Insidious Alternative Hypothesis of Trace $\text{Rh}(0)_n$ Nanoparticle Catalysis: Qualitative $\text{Hg}(0)$ Poisoning Experiments. Last, we returned to the alternative hypothesis of a putative trace $\text{Rh}(0)_n$ nanoparticle catalyst. Given the above poisoning results, $\text{Rh}(0)_n$ nanocluster catalysis is unlikely, since we previously have shown that only ~ 0.12 equiv of 1,10-phenanthroline poison is required to completely poison at least an authentic, 2–3 nm $\text{Rh}(0)_n$ nanoparticle model catalyst.^{6,26} That said, there is still the insidious alternative hypothesis here—analogue to one before⁶—that the Rh_1Cp^* , present as the dominant form of Rh, binds the 1,10-phenanthroline poison more tightly than the $\text{Rh}(0)_n$ nanoparticles. In this alternative hypothesis the $\text{Rh}(0)_n$ nanoparticle is postulated to be the true catalyst since the putative $\text{Rh}(0)_n$ is postulated to be only fractionally poisoned until all the Rh_1Cp^* present binds 1,10-phenanthroline, a hypothetical situation that could at least in principle masquerade as Rh_1Cp^* appearing to be the true catalyst based on the poisoning data. Hence, to test this final

alternative hypothesis, $\text{Hg}(0)$ poisoning studies were performed, experiments that also are of interest in revealing how the classic, qualitative $\text{Hg}(0)$ poisoning test works with putative Rh_1Cp^* , Rh_4 , and $\text{Rh}(0)_n$ -based catalysts.

In our 2005 study,¹⁰ we showed that the addition of ~ 300 equivs of $\text{Hg}(0)$ per total Rh (present initially as $[\text{RhCp}^*\text{Cl}_2]_2$), added after an active cyclohexene hydrogenation catalyst was formed and one-third of the hydrogenation reaction was complete, had no detectable effect on the catalysis (see Figure 7 in ref 10). As a check on this result, upon completion of a standard conditions cyclohexene hydrogenation beginning with $[\text{RhCp}^*\text{Cl}_2]_2$ at 22 °C and 2.7 atm initial H_2 pressure, the F-P bottle was returned to the drybox, and ~ 300 equivs of $\text{Hg}(0)$ (~ 1.7 g) per equiv of total Rh present were added to the product solution along with 1.0 mL of fresh cyclohexene. The F-P bottle was then removed from the drybox and reattached to the hydrogenation line, and a second cyclohexene hydrogenation started via pressurization with 2.7 atm of H_2 at 22 °C. The reaction solution was stirred at 600 rpm for 1.5 h, and then at 1000 rpm for an additional 8.5 h (Figure S17) while the reaction kinetics were followed in the usual way via the PC-interfaced pressure transducer. The higher, 1000 rpm stirring was used to ensure that the $\text{Hg}(0)$ fully contacts the catalyst(s), since if it does not, erroneous conclusions can be reached.¹ (The rate of hydrogenation stays essentially the same going up from 600 to 1000 rpm, thereby also ruling out the presence of any mass-transfer limitations.^{17c}) This $\text{Hg}(0)$ poisoning experiment matched our prior result¹⁰ of no detectable poisoning, a still fully active catalyst being observed that exhibited the full initial rate of $-\{d[\text{cyclohexene}]/dt\}_{\text{initial}} = 0.55 \pm 0.05$ M/h (Figure S1). This reproducible¹⁰ lack of $\text{Hg}(0)$ poisoning is consistent with, and in the context of the other evidence to this point, supporting evidence for a homogeneous, Rh_1Cp^* -based catalyst.

Finally, just to demonstrate the effect of $\text{Hg}(0)$ on an authentic sample of Rh_4 clusters (prepared from $[\text{RhCp}^*\text{Cl}_2]_2$ via a cyclohexene hydrogenation reaction at 62 °C and 3.4 atm H_2 pressure; vide supra), 300 equiv of $\text{Hg}(0)$ per total equivalents of rhodium present (~ 1.7 g) was added at standard conditions hydrogenation employing Rh_4 clusters as the catalyst at 22 °C and 2.7 atm H_2 pressure. The $\text{Hg}(0)$ poisons the Rh_4 cluster cyclohexene hydrogenation catalyst completely for over 15 h (Figure S18), which is consistent with our recent finding that Rh_4 -based catalysis of benzene hydrogenation is also fully poisoned by $\text{Hg}(0)$.⁶ The $\text{Hg}(0)$ poisoning studies further argue strongly against a Rh_4 subnanometer-based catalyst⁶ as well as a $\text{Rh}(0)_n$ nanoparticle-based catalyst,²⁷ since both are fully poisoned by $\text{Hg}(0)$, whereas the catalyst present in these studies is not. In short, only a homogeneous, Rh_1Cp^* -based catalyst is consistent with and fully supported by all of the available evidence, including these final $\text{Hg}(0)$ poisoning experiments.

CONCLUSIONS

Determination of the kinetically dominant, true catalysts derived from $[\text{RhCp}^*\text{Cl}_2]_2$ as a precatalyst for cyclohexene hydrogenation^{9,10} or benzene hydrogenation^{6,10} has proven to be a classic system, giving rise to some of the most thoroughly tested methodologies for determining the dominant catalyst in reactions beginning with discrete, organometallic precatalysts. The present work completes the $[\text{RhCp}^*\text{Cl}_2]_2$ story by carefully examining the possibility of Rh_4 subnanometer cyclohexene hydrogenation catalysis at 22 °C, 2.7 atm H_2

pressure, and with added triethylamine required for a catalytically active system.^{9,18}

The following four lines of primary, most telling, evidence provide a strong case for a Rh₁Cp*-based homogeneous catalyst as the dominant cyclohexene hydrogenation catalyst derived from [RhCp*Cl₂]₂ at 22 °C and 2.7 atm initial H₂ pressure: (i) the in operando XAFS and ¹H NMR studies that provide evidence consistent with homogeneous, Rh₁₋₂ speciation, but which also show the slow formation of Rh₄ and, thereby, raise the alternative hypothesis of Rh₄ cluster catalysis; (ii) the ex situ MS and UV-vis evidence that are confirmation Rh₁ and Rh₄ speciation, depending on the precise temperature, pressure, and concentration conditions; and importantly, (iii) the rate law obtained by Prof. Maitlis and co-workers,⁹ especially the half-order, [RhCp*Cl₂]₂^{1/2} dependence in the initial rate when starting with [RhCp*Cl₂]₂. Those kinetics imply a monomeric, Rh₁Cp*-based species as the active catalyst, one being formed from a dimeric "[RhCp*]₂",²⁸ Maitlis proposing [Rh₁Cp*(H)₂(solvent)] as the specific actual catalyst. Finally, (iv) quantitative kinetic poisoning experiments, in this case with 1,10-phenanthroline, plus qualitative Hg(0) poisoning experiments, together proved able to distinguish Rh₁Cp* from Rh₄ from Rh(0)_n active catalysts. The present example is thus another in which kinetic poisoning experiments proved crucial in disproving alternative hypotheses for the active catalyst and, thereby, in helping to provide compelling evidence for the identity of the kinetically dominant catalyst.^{6,8,29}

It is hoped that the time and effort taken with this now classic [RhCp*Cl₂]₂-based precatalyst system pioneered by Maitlis and co-workers will prove of value to others as they pursue their own studies of the "What is the true catalyst?" in their own catalytic systems. Determination of the kinetically dominant catalyst is often challenging to sometimes extremely challenging, especially if a trace component from the precatalyst leads to the kinetically dominant catalyst.^{30,31} However, because all catalytic properties of interest, be they the catalytic activity, selectivity, stability, recovery, regeneration, poisoning, or overall catalyst optimization, depend directly on the identity and nature of the actual form of the kinetically dominant catalyst, it follows that determination of the kinetically dominant catalyst is essential for catalysis to advance rationally. Hence, answering the "what is the true, kinetically dominant catalyst?" question promises to be a forefront question in catalysis for some time to come.

■ ASSOCIATED CONTENT

■ Supporting Information

The Supporting Information is available free of charge on the ACS Publications website at DOI: 10.1021/acscatal.5b00315.

Subsequent cyclohexene hydrogenation kinetics at 22 °C initially performed at 22 °C; UV-vis investigation of both first and subsequent cyclohexene hydrogenation reaction resultants; in operando XAFS and ¹H NMR investigation results; standard conditions cyclohexene hydrogenation at 26 °C; MS investigation of the resultant of standard conditions cyclohexene hydrogenation at 22 and 26 °C; 1,10-phenanthroline quantitative poisoning investigation of the resultant initially performed at 22 °C; kinetics of 1,10-phenanthroline poisoning investigation when the 1,10-phenanthroline was added to the initial solution; standard conditions

cyclohexene hydrogenation at 62 °C; subsequent cyclohexene hydrogenation kinetics at 22 °C initially performed at 62 °C; MS investigation of the resultant of standard conditions cyclohexene hydrogenation at 62 °C; 1,10-phenanthroline quantitative poisoning investigation of the resultant initially performed at 62 °C; qualitative Hg(0) poisoning experimental results of Rh₁Cp*- and Rh₄-based catalysis; standard conditions cyclohexene hydrogenation at 22 °C plus 0.5 equiv of 1,10-phenanthroline (PDF)

■ AUTHOR INFORMATION

Corresponding Authors

*E-mail: john.linehan@pnnl.gov.

*E-mail: rfinke@lamar.colostate.edu.

Present Address

[†](E.B.) Shoei Electronic Materials, Inc., 1110 NE Circle Blvd., Corvallis, OR 97330, USA.

Notes

The authors declare no competing financial interest.

■ ACKNOWLEDGMENTS

The authors would like to thank Finke Group members and Prof. Saim Özkar for their valuable input as this work was proceeding. This work was supported at Colorado State University by the U.S. Department of Energy (DOE), Office of Science, Office of Basic Energy Sciences, Division of Chemical Sciences, Geosciences & Biosciences, vial DOE Grant SE-FG402-03ER15453. The work at PNNL was also supported by the U.S. Department of Energy, Office of Science, Office of Basic Energy Sciences, Division of Chemical Sciences, Geosciences & Biosciences. Pacific Northwest National Laboratory (PNNL) is a multiprogram national laboratory operated for the DOE by Battelle. XSD/PNC facilities at the Advanced Photon Source and research at these facilities are supported by the U.S. Department of Energy, Basic Energy Sciences; a Major Resources Support Grant from NSERC; the University of Washington; the Canadian Light Source; and the Advanced Photon Source. Use of the Advanced Photon Source, an Office of Science User Facility operated for the U.S. Department of Energy Office of Science by Argonne National Laboratory was supported by the U.S. DOE under Contract No. DE-AC02-06CH11357.

■ REFERENCES

- (1) Widegren, J. A.; Finke, R. G. *J. Mol. Catal. A: Chem.* **2003**, *198*, 317–341.
- (2) Crabtree, R. H. *Chem. Rev.* **2012**, *112*, 1536–1554.
- (3) Phan, N. T. S.; Sluys, M. V. D.; Jones, C. W. *Adv. Synth. Catal.* **2006**, *348*, 609–679.
- (4) Alley, W. M.; Hamdemir, I. K.; Johnson, K. A.; Finke, R. G. *J. Mol. Catal. A: Chem.* **2010**, *315*, 1–27.
- (5) de Vries, J. G. *Dalton Trans.* **2006**, 421–429.
- (6) Bayram, E.; Linehan, J. C.; Fulton, J. L.; Roberts, J. A. S.; Szymczak, N. K.; Smurthwaite, T. D.; Özkar, S.; Balasubramanian, M.; Finke, R. G. *J. Am. Chem. Soc.* **2011**, *133*, 18889–18902.
- (7) Tinnemans, S. J.; Mesu, J. G.; Kervinen, K.; Visser, T.; Nijhuis, T. A.; Beale, A. M.; Keller, D. E.; van der Eerden, A. M. J.; Weckhuysen, B. M. *Catal. Today* **2006**, *113*, 3–15.
- (8) Bayram, E.; Finke, R. G. *ACS Catal.* **2012**, *2*, 1967–1975.
- (9) Gill, D. S.; White, C.; Maitlis, P. M. *J. Chem. Soc., Dalton Trans.* **1978**, 617–626.

(10) Hagen, C. M.; Widegren, J. A.; Maitlis, P. M.; Finke, R. G. *J. Am. Chem. Soc.* **2005**, *127*, 4423–4432.

(11) Collman, J. P.; Kosydar, K. M.; Bressan, M.; Lamanna, W.; Garrett, T. *J. Am. Chem. Soc.* **1984**, *106*, 2569–2579.

(12) Sonnenberg, J. F.; Coombs, N.; Dube, P. A.; Morris, R. H. *J. Am. Chem. Soc.* **2012**, *134*, 5893–5899.

(13) Lin, Y.; Finke, R. G. *J. Am. Chem. Soc.* **1994**, *116*, 8335–8353.

(14) Özkar, S.; Finke, R. G. *J. Am. Chem. Soc.* **2002**, *124*, 5796–5810.

(15) Özkar, S.; Finke, R. G. *Langmuir* **2002**, *18*, 7653–7662.

(16) Lin, Y.; Finke, R. G. *Inorg. Chem.* **1994**, *33*, 4891–4910.

(17) (a) Watzky, M. A.; Finke, R. G. *J. Am. Chem. Soc.* **1997**, *119*, 10382–10400. (b) Watzky, M. A.; Finke, R. G. *Chem. Mater.* **1997**, *9*, 3083–3095. (c) Aiken, J. D., III; Finke, R. G. *J. Am. Chem. Soc.* **1998**, *120*, 9545–9554. (d) Widegren, J. A.; Aiken, J. D., III; Özkar, S.; Finke, R. G. *Chem. Mater.* **2001**, *13*, 312–324.

(18) In Maitlis's 1978 paper,⁹ triethylamine was reported as an important additive for the generation of the active catalyst. As a control experiment herein, a standard conditions cyclohexene hydrogenation without any added triethylamine yielded no activity whatsoever (as reported also by Maitlis⁹) over the 10 h the reaction was followed, thereby confirming the requirement for an added base such as triethylamine, presumably for the heterolytic activation of hydrogen.

(19) (a) Fulton, J. L.; Linehan, J. C.; Autrey, T.; Balusbramanian, M.; Chen, Y.; Szymczak, N. K. *J. Am. Chem. Soc.* **2007**, *129*, 11936–10949. (b) Rousseau, R. J.; Schenter, G. K.; Fulton, J. L.; Linehan, J. C.; Englehard, M. H.; Autrey, T. *J. Am. Chem. Soc.* **2009**, *131*, 10516–10524.

(20) Stern, E. A.; Newille, M.; Ravel, B.; Yacoby, Y. *Phys. B: Condens. Matter* **1995**, *208/209*, 117–120.

(21) (a) Yonker, C. R.; Linehan, J. C. *J. Organomet. Chem.* **2002**, *650*, 249–257. (b) Yonker, C. R.; Linehan, J. C. *Prog. Nucl. Magn. Reson. Spectrosc.* **2005**, *47*, 95–109.

(22) A control experiment consisting of a standard conditions cyclohexene hydrogenation beginning with $[\text{RhCp}^*\text{Cl}_2]_2$ at 22 °C and 2.7 atm initial H_2 pressure with 2 mL of cyclohexene (instead of 1 mL of cyclohexene) did not show biphasic hydrogenation kinetics. This result implies that the biphasic kinetics and associated catalyst deactivation are valid only for the second, subsequent cyclohexene hydrogenation.

(23) Chifotides, H. T.; Dunbar, K. R. In *Multiple Bonds Between Metals*, 3rd ed.; Cotton, F. A., Murillo, C. A., Walton, R. A., Eds.; Springer: New York, 2005; p 465.

(24) Maitlis, P. M. *Acc. Chem. Res.* **1978**, *11*, 301–307.

(25) A control reaction performed by adding 0.5 equiv of 1,10-phenanthroline to the initial solution, that is, beginning with $[\text{RhCp}^*\text{Cl}_2]_2$ rather than with the evolved catalyst, exhibited cyclohexene hydrogenation kinetics completely different from those obtained under standard conditions, as shown in Figure 1, for example; see the [Supporting Information](#), Figure S19. Hence, it is important to evolve the catalyst first before adding the poison.

(26) Similarly, only 0.18 equiv of CS_2 per total Rh is required to poison the polyoxoanion-stabilized $\text{Rh}(0)_n$ nanoparticles as described in Hornstein, B. J.; Aiken III, J. D.; Finke, R. G. *Inorg. Chem.* **2002**, *41*, 1625–1638.

(27) Aiken, J. D., III; Finke, R. G. *Chem. Mater.* **1999**, *11*, 1035–1047.

(28) Note that the precise ligation of the dimeric $[\text{RhCp}^*]_2$ remains somewhat uncertain; the available evidence (including our in operando XAFS showing a loss of Rh-Cl from the $[\text{RhCp}^*\text{Cl}_2]_2$ starting complex) is most consistent with the formation of some dimeric, but perhaps also $\text{RhCp}^*\text{O}-i\text{Pr}$ containing, species. We thank a referee for raising this possibility and for other valuable comments.

(29) Sonnenberg, J. F.; Morris, R. A. *Catal. Sci. Technol.* **2014**, *4*, 3426–3438.

(30) The case of water-oxidation catalysis is currently a very active area in which the identification of the kinetically dominant catalyst can be quite challenging, in part because 58 μM to 100s of nM leached

metals, from precatalysts that might appear to be “stable” by many physical methods, are actually not 100% stable and degrade when quantitative experiments are done to detect that degradation. See: (a) Stracke, J. J.; Finke, R. G. *ACS Catal.* **2014**, *4*, 909–933. (b) Stracke, J. J.; Finke, R. G. *J. Am. Chem. Soc.* **2011**, *133*, 14872–14875. (c) Stracke, J. J.; Finke, R. G. *ACS Catal.* **2013**, *3*, 1209–1219. (d) Stracke, J. J.; Finke, R. G. *ACS Catal.* **2014**, *4*, 79–89.

(31) The following, important work suggests that a mere 70 ppb of Co^{2+} impurity can carry the observed water-oxidation catalysis activity assigned previously to Co_4O_4 cubane clusters: (a) Ullman, A. M.; Liu, Y.; Huynh, M.; Bediako, D. K.; Wang, H.; Anderson, B. L.; Powers, D. C.; Breen, J. J.; Abruña, H. D.; Nocera, D. G. *J. Am. Chem. Soc.* **2014**, *136*, 17681–17688.